Available online at www.sciencedirect.com
ScienceDirect
Biochemical and Biophysical Research Communications 349 (2006) 439–448
BBRC
www.elsevier.com/locate/ybbrc

Hepatic knockdown of mitochondrial GPAT1 in *ob*/*ob* mice improves metabolic profile

Haiyan Xu [a,*], Denise Wilcox [a], Phong Nguyen [a], Martin Voorbach [a], Thomas Suhar [a], Sheryl J. Morgan [b], W. Frank An [c], Lin Ge [c], Jack Green [c], Zhidan Wu [c], Ruth E. Gimeno [c], Regina Reilly [a], Peer B. Jacobson [a], Christine A. Collins [a], Katherine Landschulz [a], Terry Surowy [a]

[a] *Metabolic Disease Research, Abbott Laboratories, Abbott Park, IL 60064, USA*
[b] *Global Preclinical Safety, Abbott Laboratories, Abbott Park, IL 60064, USA*
[c] *Millennium Pharmaceuticals Inc., Cambridge, MA 02139, USA*

Received 14 August 2006
Available online 22 August 2006

Abstract

Glycerol-3-phosphate acyltransferase (GPAT) controls the first step of triglyceride (TAG) synthesis. Three distinct GPAT activities have been identified, two localized in mitochondria and one in microsomes. Mitochondrial GPAT1 (mtGPAT1) is abundantly expressed in the liver and constitutes approximately 50% of total GPAT activities in this organ. Hepatic mtGPAT1 activity is elevated in obese rodents. Mice deficient in mtGPAT1 have an improved lipid profile. To investigate if beneficial effects can result from reduced hepatic expression of mtGPAT1 in adult obese mice, adenoviral vector-based short hairpin RNA interference (shRNA) technology was used to knockdown mtGPAT1 expression in livers of *ob*/*ob* mice. Reduced expression of mtGPAT1 mRNA in liver of *ob*/*ob* mice resulted in dramatic and dose dependent reduction in mtGPAT1 activity. Reduced hepatic TAG, diacylglycerol, and free fatty acid, as well as reduced plasma cholesterol and glucose, were also observed. Fatty acid composition analysis revealed decrease of C16:0 in major lipid species. Our results demonstrate that acute reduction of mtGPAT1 in liver of *ob*/*ob* mice reduces TAG synthesis, which points to a role for mtGPAT1 in the correction of obesity and related disorders.

Keywords: mtGPAT1; *ob*/*ob* mice; Obesity; RNA interference; Adenovirus

Obesity, currently affecting one-third of the adult population in the United States, has become an epidemic disease in developed countries and is also increasing at an alarming rate in developing nations [1]. Obesity has been identified as a major risk factor for the development of many life threatening diseases, such as type 2 diabetes, insulin resistance, dyslipidemia, atherosclerosis, hypertension, and non-alcoholic fatty liver disease (NAFLD)-related cirrhosis [2]. This is an area of tremendous medical need and new therapeutic agents are necessary to address a variety of the pathophysiological processes of this disorder.

Liver is a key organ for regulating transient energy fluctuations through regulation of lipid and carbohydrate metabolism to meet the body's needs. Dysregulation of lipid metabolism in the liver contributes significantly to the development of obesity related dyslipidemia and NAFLD. The liver handles fatty acids derived from diet and is also an important site for *de novo* lipogenesis. A critical regulator of lipogenesis is GPAT, which catalyzes the first and most likely rate-limiting step of TAG synthesis [3]. In the liver, the glycerol-3-phosphate pathway is the major route for esterification of free fatty acids derived from both diet

* Corresponding author. Present address: Brown Medical School, Hallett Center for Diabetes and Endocrinology, Providence, RI 02903, USA. Fax: +1 401 444 3784.
E-mail address: haiyan_xu@brown.edu (H. Xu).

0006-291X/$ - see front matter © 2006 Elsevier Inc. All rights reserved.
doi:10.1016/j.bbrc.2006.08.071

and *de novo* lipogenesis [4]. Three biochemically distinct GPAT activities have been identified so far, including one microsomal and two mitochondrial enzymes [5,6]. The gene encoding mtGPAT1 is highly expressed in both liver and adipose tissue [7,8]. Activity of mtGPAT1 can be differentiated from the remaining two GPATs by its resistance to *N*-ethylmaleimide (NEM), a sulfhydryl group reactive reagent [6,9]. In most tissues, mtGPAT1 makes up less than 10% of total GPAT activity. In the liver, however, mtGPAT1 accounts for about 50% of total GPAT activity [10]. The mitochondrial GPAT1 activity is highly regulated by nutrients and hormones in contrast to microsomal GPAT activity [3,9,10], indicating the importance of mtGPAT1 as a sensor/regulator of lipid biosynthesis in response to changes in nutritional state.

There is a growing body of evidence to show that the activity of mtGPAT1 is upregulated in multiple tissues in obese animals, including liver [11], adipose tissue [12], intestine [12], and pancreatic β-cells [13], when compared to the activity in lean animals. *In vitro* studies have demonstrated that mtGPAT1 is important for directing the metabolic fate of exogenous fatty acids in hepatocytes [14]. Overexpression of mtGPAT1 in hepatocytes increased TAG synthesis and decreased fatty acid oxidation [11,14]. Heterologous expression of mtGPAT1 in other cell types also caused increased TAG synthesis [15]. Mitochondrial GPAT1 is localized to the outer membrane of mitochondria [16] and could compete for substrates with carnitine palmitoyl transferase 1 (CPT1), the rate-limiting enzyme for fatty acid oxidation. In addition, mtGPAT1 and CPT1 are reciprocally regulated by AMP-activated kinase [17,18], a key energy sensor that changes metabolism to meet the needs for energy utilization. Consistent with evidence from *in vitro* studies, the pivotal role of mtGPAT1 in control of the balance between fat storage and fatty acid oxidation has been confirmed in both gain-of-function and loss-of-function animal models. Liver-specific overexpression of mtGPAT1 in lean mice resulted in hepatic steatosis, increased TAG secretion, and reduced fatty acid oxidation [19]. Consistent with this, mtGPAT1 knockout mice have reduced liver TAG levels and increased plasma β-hydroxybutyrate levels as well as increased plasma levels of acyl carnitines when placed on a high fat/high sucrose diet or a high oil diet [20–22], suggesting reduced partitioning of fatty acid into TAG synthesis and increased β-oxidation. Given the possible differences in phenotype between genetic global knockout animals and acute pharmacological intervention, we sought to assess the role of mtGPAT1 in liver lipid metabolism in adult obese mice by using an adenovirus-mediated shRNA knockdown approach. Our studies show that acute reduction of mtGPAT1 in mtGPAT1 livers of *ob/ob* mice resulted in reduced liver TAG level and content of C16:0, consistent with the phenotype observed in mtGPAT1 knockout mice.

Materials and methods

Construction of shRNA expression vectors and preparation of recombinant adenovirus. Seven short hairpin oligonucleotides and complementary strands were designed to specifically target mouse mtGPAT1. The BLOCK-iT™ RNAi system (Invitrogen, Carlsbad, CA) was used for shRNA construction. To evaluate the potency of these shRNAs *in vitro*, a partial mtGPAT1 cDNA (corresponding to nucleotides 433–1293, residues 144–431 of NM_008149) which contains the sequence targeted by all shRNAs was fused in-frame to EGFP cDNA in the pEGFP-N1 vector (BD Biosciences, Mountain View, CA). In order to generate the recombinant adenovirus vectors expressing shRNAs for mtGPAT1, selected pENTR/U6-shRNA plasmids were recombined into the Gateway-based pAd-BLOCK-iT DEST™ vector (Invitrogen, Carlsbad, CA), according to the manufacturer's instructions. As a negative control, a recombinant adenovirus vector expressing a shRNA directed against GFP was generated. The sequences of GFP-shRNA and effective mtGPAT1-shRNA1, 4, and 6 are shown below:

GFP-shRNA
Top: 5′ caccGAAGCAGCACGACTTCTTCttcaagagaGAAGAAGTCGTGCTGCTTC
Bottom: 5′ aaaaGAAGCAGCACGACTTCTTCtctcttgaaGAAGAAGTCGTGCTGCTTC
mtGPAT1-shRNA1
Top: 5′ caccGACGGAGGCTCGATGAAACttcaagagaGTTTCATCGAGCCTCCGTC
Bottom: 5′ aaaaGACGGAGGCTCGATGAAACtctcttgaaGTTTCATCGA GCCTCCGTC
mtGPAT1-shRNA4
Top: 5′ caccTACATCGCCTCGGGCAATAttcaagagaTATTGCCCGAGGCGATGTA
Bottom: 5′ aaaaTACATCGCCTCGGGCAATAtctcttgaaTATTGCCCGA GGCGATGTA
mtGPAT1-shRNA6
Top: 5′ caccGCATCTCGTATGATCGCATttcaagagaATGCGATCATACG AGATGC
Bottom: 5′ aaaaGCATCTCGTATGATCGCATtctcttgaa ATGCGATCATACGAGATGC

Immunoblot analysis. To assay the efficacy of mtGPAT1-shRNAs, human HEK293A cells co-transfected with plasmids expressing mtGPAT1-shRNAs and mtGPAT1-EGFP fusion protein were harvested and 60 μg of protein from each cell lysate was used for immunoblot analysis. Briefly, following SDS–PAGE, the resolved proteins were transferred onto PVDF membranes. Membranes were blocked in 5% non-fat dried milk in Tris-buffered saline containing 0.5% Tween 20 (TBST) for 1 h, then incubated with rabbit polyclonal antibodies for GFP (Santa Cruz Biotechnology Inc., Santa Cruz, CA) at a 1:100 dilution in 5% non-fat dried milk/TBST. After four washings in TBST, membranes were incubated with biotinylated goat anti-rabbit IgG (Kirkegaard & Perry Laboratories, Gaithersburg, MD) for 1 h at the dilution of 1:4000. Finally, streptavidin-labeled horseradish peroxidase (HRP, Kirkegaard & Perry Laboratories, Gaithersburg, MD) was used at 1:100 for 45 min to detect signal.

Glycerol uptake assay. Primary hepatocytes isolated from male B6.V-Lep *ob/ob* mice were seeded on 24-well plates at a density of 2×10^5/well and 24 h later were infected with adenovirus expressing shRNA against mtGPAT1 at multiplicity of infection (MOI) 50. Twenty-four hours after infection, the cells were incubated overnight in serum-free DMEM supplemented with 0.5% bovine serum albumin. Forty-eight hours after infection, cells were rinsed once with Krebs–Ringer buffer and then incubated with 500 μl Krebs–Ringer buffer supplemented with 5 mM glucose, 0.5% BSA, and [^{3}H]-glycerol (American Radiolabelled Chemical, Inc., St. Louis, MO) at a final concentration of 1 μCi/ml (approximately 50 nM) at 37 °C for 5 h. Cells were washed four times with cold Krebs–Ringer buffer and lysed with 150 μl of 1 0.1% SDS solution. Radioactivity was counted by using 50 μl of cell lysate and total counts were normalized by protein content.

RNA isolation and quantitative RT-PCR analysis. RNA samples were extracted using the TRIZOL®reagent (Invitrogen, Carlsbad, CA) for real-time PCR analysis. The relative mRNA expression levels were normalized to expression of 28S rRNA. The sequences for the primers and probe sets are as follows:

mtGPAT1
Forward: 5′ GTCCTGCGCTATCATGTCCA
Reverse: 5′ GGATTCCCTGCCTGTGTCTG
Probe: 5′ CCACATTGTGGCCTGTCTGCTCCT
mACO1
Forward: 5′ GAGTGAGCTGCCTGAGCTTCA
Reverse: 5′ TCTTCGATACCAGCATTGGCT
Probe: 5′ AGCTGGGCTGAAGGCTTTTACTACCTGGA
mCPT-1a
Forward: 5′ CGCGCTCTTAGGACTACTTGCTA
Reverse: 5′ GAGACCTGAGAGAGGAATGTCACA
Probe: 5′ CTGTTACTCGGAGTATTCCTGCTAGTAC
mCPT II
Forward: 5′ CTCCTCCTACTCAGGACGCAAT
Reverse: 5′ CATCGAACATGTCTTCCAAGCA
Probe: 5′ CCCGAGAGTTTCTCCACTGTGTCCAGA

Animal protocols and blood chemistries. All animal protocols used in this study were approved by the Abbott Institutional Animal Care and Use Committee. Male B6.V-Lep *ob*/*ob* mice were purchased from Jackson Laboratories (Bar Harbor, ME) and received at the age of 5–6 weeks. Mice were individually housed in micro-isolator cages one week prior to the studies for acclimation. Mice were culled into experimental groups of equivalent average postprandial glucose level and body weight at the beginning of the study. Treated animals underwent a single 150 μl tail injection of vehicle or recombinant adenovirus expressing shRNA against GFP or mtGPAT1. Body weight, food intake, and postprandial glucose levels (Precision PCx, Abbott Laboratories, Abbott Park, IL) were measured 5 days post injection prior to euthanization. For measurement of β-hydroxybutyrate levels, a subset of mice were fasted overnight and blood was collected for assay. At the end of studies, mice were euthanized by CO_2 inhalation under fed condition for blood and tissue collection. Plasma TAG (Infinity kits, Thermo Electron Corporation, Louisville, CO), cholesterol (Infinity kits, Thermo Electron Corporation, Louisville, CO), free fatty acids (WACO Chemicals, Germany), insulin (APLCO Diagnostics, Windham, NH), β-hydroxybutyrate (Precision Xtra meter, Abbott Laboratories, Abbott Park, IL), and ALT/AST (Sigma Diagnostics, St. Louis, MO) were measured according to manufacturer's instructions.

Isolation of mitochondria and GPAT activity assay. Primary hepatocytes or approximately one-third of fresh mouse liver was homogenized using a Dounce homogenizer in ice-cold homogenization buffer containing 10 mM Tris–HCl, pH 7.4, 250 mM sucrose, 1 mM dithiothreitol, 1 mM EDTA and Complete™, EDTA-free proteinase inhibitor cocktail tablets (Roche Applied Science, Nutley, NJ). Membrane debris and nuclei were removed by centrifugation at 600*g* at 4 °C for 5 min. Supernatant was transferred to clean tubes and centrifuged at 10,000*g* at 4 °C for 10 min to pellet mitochondria. The pellet was then resuspended with ice-cold homogenization buffer for protein quantification and enzymatic assay. Prior to assay of mtGPAT1 activity, the mitochondrial suspension was incubated on ice for 15 min in the presence of 2 mM *N*-ethylmaleimide (Sigma Chemicals, St. Louis, MO) to inactivate other GPAT activities. Mitochondrial GPAT activities were assayed, at steady state equilibrium conditions, using 10 μg of protein at 25 °C for 1 h in assay buffer (75 mM Tris–HCl, pH 7.4, 4 mM $MgCl_2$, and 8 mM NaF) containing 100 μM palmitoyl-CoA (Avanti Polar Lipids, Alabaster, AL), 1 mM glycerol-3-phosphate (Sigma Chemicals, St. Louis, MO), 2 mg/ml BSA and 1 μCi [^{3}H]-glycerol-3-phosphate (American Radiolabeled Chemical, Inc., St. Louis, MO). The reaction was stopped by adding five volumes of water-saturated 1-butanol. After thorough mixing to extract the lysophosphatidic acid product, phase separation was achieved by centrifugation at 13,000*g* in a microcentrifuge for 10 min. The aqueous phase was transferred to clean tubes and further separation was achieved using two back-extractions with water-saturated 1-butanol. The top layer was then transferred to a scintillation vial and counted for radioactivity.

Hepatic lipid analysis. Approximately 100 mg each of snap-frozen and pulverized liver samples were provided to Lipomics Technology, Inc. for lipid profile analysis. In-house, liver TAG was determined using a method based on measurement of glycerol released from triglycerides. Briefly, approximately 100 mg of liver tissue was homogenized in thirty volumes of ethanol. Cell debris was allowed to settle, and further clarification was achieved by centrifugation of the supernatant at 15,000*g* for 10 min at room temperature. Assay of TAG was performed using a 96-well format. Samples were diluted 1:5 for assay. For standards, Lipid Lin-Trol standards were used (Sigma Chemicals, St. Louis, MO). For both standards and samples, 24 volumes of Infinity Triglyceride Reagent (Thermo Electron Corporation, Louisville, CO) were added and samples were incubated at 37 °C for 5 min. After cooling down to room temperature, absorbance of samples was read at 520 nm.

Statistical analysis. The Student's *t*-test was used to compare the difference between animals treated with adenovirus expressing shRNA against mtGPAT1 and shRNA against GFP.

Results

Construction of shRNAs against mtGPAT1 and knockdown in vitro in hepatocytes

Seven shRNAs were designed to specifically target mouse mtGPAT1. Efficacy in knocking down mtGPAT1 was assayed by co-transfecting mtGPAT1-EGFP expression construct and each of these shRNA plasmids into HEK293A cells. Immunoblot analysis was performed to examine the expression level of the fusion protein using an antibody against GFP (Fig. 1A). The expression level of the mtGPAT1-EGFP fusion protein was reduced to undetectable levels when co-transfected with shRNAs 1 and 6, and was barely detectable with shRNA 4. These three shRNAs were then recombined into a Gateway-based adenovirus destination vector. Recombinant adenoviruses containing the chosen shRNAs were used to infect primary mouse hepatocytes isolated from lean C57BL/6J mice, to evaluate the efficiency to knockdown endogenous mtGPAT1. At a multiplicity of infection (MOI) of 50, recombinant adenovirus expressing shRNA1 was the most potent among the three tested, knocking down endogenous mtGPAT1 mRNA by 98% (Fig. 1B). Recombinant adenoviruses expressing shRNAs 4 and 6 were less potent, knocking down mtGPAT1 mRNA by 56% and 81%, respectively, under the same condition. Based on these results, shRNA1, designated as mtGPAT1-shRNA1, was chosen for all experiments.

A series of *in vitro* experiments were performed using primary hepatocytes isolated from *ob*/*ob* mice to further evaluate the effect of mtGPAT1 mRNA knockdown on mtGPAT1 enzymatic activity and lipogenesis. Recombinant adenovirus expressing mtGPAT1-shRNA1 effectively knocked down the endogenous mtGPAT1 mRNA to undetectable level in primary *ob*/*ob* hepatocytes (Fig. 2A). The decrease of mtGPAT1 mRNA was accompanied by a 70% decrease in NEM-resistant mtGPAT1 enzymatic activity (Fig. 2B). In contrast, NEM-sensitive GPAT activity in the mitochondrial preparation was not significantly

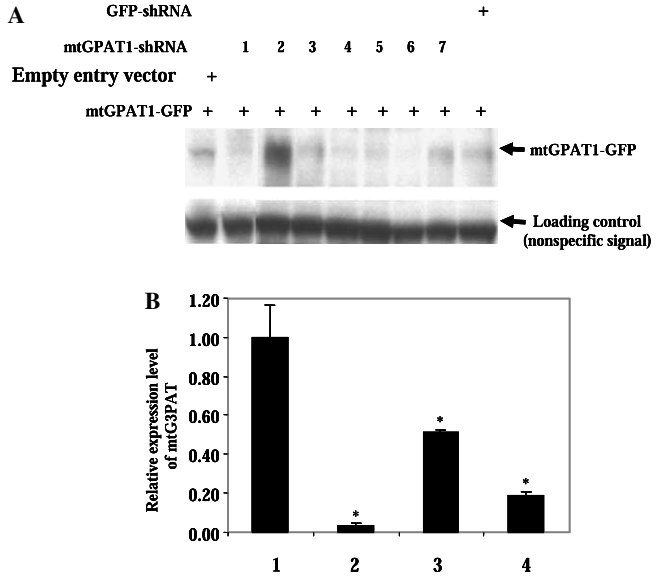

Fig. 1. Selection of shRNAs for knockdown of mtGPAT1. (A) Seven short hairpin intefering RNAs (shRNA) against mtGPAT1 were designed and cloned into an Invitrogen Gateway-based entry vector under the control of the human U6 promoter. A shRNA against GFP was used as a control. To test the knockdown efficiency, the entry vectors containing different hairpins were co-transfected with a vector expressing mtGPAT1-EGFP fusion protein into HEK293A cells. Western analysis was performed after 48 h to assess the expression level of mtGPAT1-EGFP using an antibody against GFP. (B) shRNA 1, 4, and 6 were selected and recombined into a Gateway-based adenovirus vector. Purified viruses containing the shRNA against GFP (lane 1) or shRNAs against mtGPAT1(lanes 2–4) were used to infect primary hepatocytes isolated from C57BL/6J mice and effect was assessed by quantitative PCR 48 h after infection. Data shown are representative of three independent experiments. Student's *t*-test was used to compare statistical differences between shRNAs against mtGPAT1 and shRNA against GFP. $^{*}P < 0.05$.

altered (Fig. 2C) by shRNA treatment. Reductions in hepatocyte mtGPAT1 activity and mRNA were accompanied by significant changes in glycerolipid synthesis: a 42% decrease in glycerol uptake was observed in *ob/ob* hepatocytes infected with the recombinant adenovirus expressing mtGPAT1-shRNA1 compared to the cells infected with recombinant adenovirus expressing GFP-shRNA (Fig. 2D).

Hepatic mtGPAT1 knockdown in ob/ob mice and metabolic profiling

To further understand the importance of mtGPAT1 in metabolism, particularly hepatic glycerolipid synthesis, recombinant adenovirus expressing mtGPAT1-shRNA1 was injected into *ob/ob* mice. This enabled us to examine effects of lowering mtGPAT1 enzymatic activity in an obese and diabetic animal model. A single tail-vein injection was used to deliver recombinant adenovirus at two doses, 2×10^8 and 1×10^9 pfu per mouse. Effects of mtGPAT1 knockdown were examined 5 days after injection. Control animals were treated in parallel with vehicle or with recombinant adenovirus expressing GFP-shRNA. In agreement with other published studies using adenovirus, our recombinant adenovirus constructs were delivered predominantly to liver (data not shown). Five days after injection, the hepatic mRNA level of mtGPAT1 was decreased by 51% in the low dose group and was undetectable in the high dose group (Fig. 3A). Consistent with decreased mtGPAT1 mRNA levels, hepatic mtGPAT1 enzymatic activity was also reduced by targeted shRNA treatment. Compared to GFP-shRNA treated animals, the activity of mtGPAT1

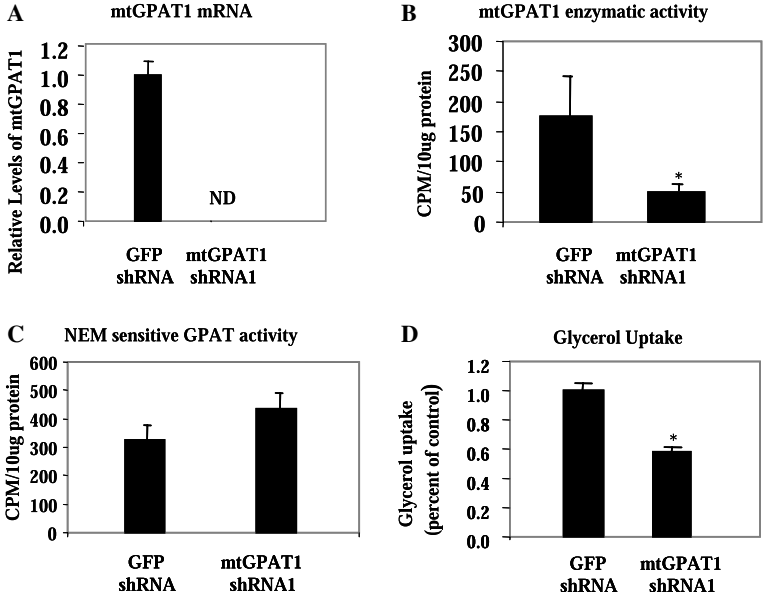

Fig. 2. Effects of knocking down mtGPAT1 in primary hepatocytes. Hepatocytes isolated from *ob/ob* mice were infected with either control virus containing shRNA against GFP or shRNA 1 against mtGPAT1. Mitochondrial GPAT1 mRNA (A) and enzymatic activity (B) were examined 48 h after infection. NEM-sensitive GPAT activity was also determined (C) with the same mitochondria preparation used for examination of mtGPAT1 activity. Glycerol uptake by hepatocytes was examined 48 h after infection (D). Data shown are representative of at least three independent experiments. Student's *t*-test was used to compare statistical differences between hepatocytes infected with mtGPAT1-shRNA1 versus GFP-shRNA. ND, not detectable; $^{*}P < 0.05$.

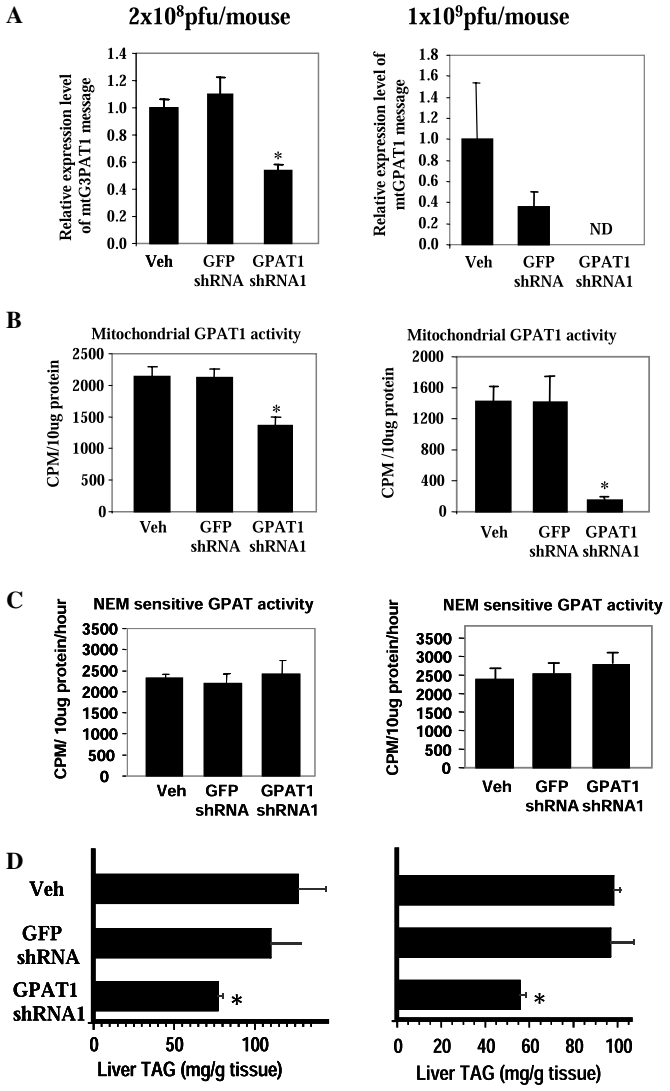

Fig. 3. Effects of knocking down mtGPAT1 in *ob*/*ob* mice. Adenovirus containing shRNA against GFP or mtGPAT1 was injected into *ob*/*ob* mice at two doses via tail vein: 2×10^8 pfu/mouse (left panels) and 1×10^9 pfu/mouse (right panels). Five days post injection, mice were sacrificed and livers were taken to examine mtGPAT1 mRNA (A) and activity (B). NEM-sensitive GPAT activities (C) were also assessed to demonstrate specific inhibition of NEM-resistant mtGPAT1 activity. Liver TAG levels were measured to evaluate alteration of hepatic lipid metabolism (D). Student's *t*-test was used to compare statistical differences between liver samples from mice injected with mtGPAT1-shRNA1 and GFP-shRNA, $n = 5$ per group. $^*P < 0.05$; ND, not detectable.

was reduced by 36% and 90%, respectively, in low and high dose animal groups treated with mtGPAT1-shRNA1 (Fig. 3B). The activity of NEM-sensitive GPAT was not reduced, supporting specific knockdown of mtGPAT1 activity and not other GPAT activity (Fig. 3C). Liver TAG content was directly affected by shRNA-mediated knockdown of mtGPAT1. Mice treated with recombinant adenovirus expressing mtGPAT1-shRNA1 showed a 30% reduction of liver TAG levels in the low dose group and a 42% reduction in the high dose group compared to mice treated with recombinant adenovirus expressing GFP-shRNA (Fig. 3D). No statistically significant difference in liver TAG levels was observed between vehicle treated and GFP-shRNA treated mice, suggesting that the reduction of liver TAG is specifically related to mtGPAT1 knockdown.

Other than lowered liver TAG levels, there were no other significant findings observed in the low dose (2×10^8 pfu/mouse) mtGPAT1-shRNA1 treated animals compared to GFP-shRNA treated control animals. This included no changes in plasma FFAs, plasma TAG, plasma cholesterol, plasma insulin, blood glucose, body weight or food intake (Table 1). In contrast, animals treated with high dose (1×10^9 pfu/mouse) mtGPAT1-shRNA1 for 5 days had, additionally, a 30% reduction in plasma glucose level and a 35% reduction in total plasma cholesterol level, compared to equivalently dosed GFP-shRNA treated mice (Table 1). Further classification of plasma cholesterol revealed that the reduction of cholesterol is entirely due to decreased level of cholesterol ester without change of free cholesterol (Table 1). These additional changes presumably reflect early impact of more-extensively lowered mtGPAT1 activity. Importantly, no significant change in liver function, assessed by examining circulating AST and ALT levels, was observed as result of adenovirus delivery in either low dose or high dose adenovirus-treated mice within a 5-day time frame (Table 1). To understand whether reduced liver TAG is simply due to decreased lipid synthesis or also involves increased fatty acid oxidation, plasma β-hydroxybutyrate levels were measured in the 5-day high dose study, but did not show significant changes (Table 1). Possibilities of increased hepatic peroxisomal and mitochondrial fatty acid oxidation were also explored by examining expression levels of acyl CoA oxidase 1 (ACO1), carnitine palmitoyltransferase I (CPT I), and carnitine palmitoyltransferase II (CPT II). ACO1 is a key enzyme controlling peroxisomal oxidation and its transcriptional regulation corresponds to rate of peroxisomal oxidation. CPT I is a rate-limiting enzyme of mitochondrial oxidation and controls conversion of fatty acyl CoAs to acyl carnitines. CPT II converts acyl carnitines back to acyl CoAs. The expression levels of these three genes were not changed in livers of mtGPAT1 knockdown *ob*/*ob* mice (Table 2), indicating that reduced liver TAG is caused by decreased lipogenesis.

Effects of mtGPAT1 knockdown on hepatic lipid content and composition

To investigate other changes in hepatic lipids that may have occurred in addition to the reduction of TAG content seen with mtGPAT1 knockdown, lipid profiling was performed with liver samples from the high dose group animals treated with recombinant adenovirus expressing mtGPAT1-shRNA1 and compared to liver samples from *ob*/*ob* mice receiving recombinant adenovirus expressing GFP-shRNA. Levels of diacylglycerol (DAG) were significantly reduced by 51%, and total free fatty acid levels (FFAs) were reduced by

Table 1
Metabolic profiling of mtGPAT1 knockdown and control mice

	FFAs (mM)	TAG (mg/dL)	Cholesterol (mg/dL)	Insulin (ng/ml)	Glucose (mg/dL)	Weight (g)	FI (g)	β-OH (mg/dL)	AST (mg/dL)	ALT (mg/dL)
2×10^8 pfu										
Untreated	0.82 ± 0.17	157 ± 51	183 ± 14	17 ± 5.7	334 ± 49	51 ± 1.9	33 ± 0.8	N/A	271 ± 12	528 ± 20
Vehicle	0.87 ± 0.16	144 ± 14	177 ± 10	14 ±2.5	334 ± 49	51 ± 1.9	33 ± 0.8	N/A	246 ± 41	577 ± 22
GFP-shRNA	0.79 ± 0.15	171 ± 20	191 ± 14	13 ±2.9	376 ± 43	49 ± 0.7	34 ± 1.7	N/A	238 ± 36	547 ± 63
mtGPAT1 shRNA	0.80 ± 0.12	188 ± 22	203 ± 19	12 ± 1.6	327 ± 72	50 ± 2.3	28 ± 2.3	N/A	297 ± 41	451 ± 41
1×10^9 pfu										
Vehicle	0.49 ± 0.05	370 ± 49	476 ± 24	9.2 ± 1.2	381 ± 27	45.6 ± 1.0	43.6 ± 2.1	0.38 ± 0.1	305 ± 30	654 ± 40
GFP-shRNA	1.00 ± 0.15	431 ± 44	552 ± 45	5.7 ± 0.7	394 ± 22	45.3 ± 0.7	39.5 ± 1.2	0.34 ± 0.07	341 ± 26	627 ± 43
mtGPAT1 shRNA	0.70 ± 0.05	396 ± 41	359 ± 48*	12 ± 1.7*	277 ± 37*	45.1 ± 0.72	35.9 ± 2.3	0.38 ± 0.04	412 ± 29	609 ± 14
	Cholesterol ester (nmol/gram plasma)	Free cholesterol (nmol/gram plasma)								
1×10^9 pfu										
Vehicle	2310.5 ± 132	1004 ± 43.4								
GFP-shRNA	2706.7 ± 242	1102 ± 107								
mtGPAT1 -shRNA	1587.4 ± 107*	1059 ± 104								

Five to thirteen mice were used for each analysis. Values are presented as means ± standard errors. Student's *t*-test was used to compare statistical differences between liver samples from mice injected with mtGPAT1-shRNA1 and GFP-shRNA. *$P < 0.05$. β-OH, β-hydroxybutyrate; FI, accumulative food intake over the entire experimental period.

48.5% (Fig. 4). This provides additional novel information to that reported in global mtGPAT1 knockout mice. In contrast, hepatic cholesterol ester (CE) and phospholipid contents, including phosphatidylcholine (PC), phosphatidylethanolamine (PE), phosphatidylserine (PS), lysophosphatidylcholine (LYPC), sphingomyelin (SM), and cardiolipin (CL) were unchanged with reduction of liver mtGPAT1 expression (Fig. 4).

Changes in fatty acid composition have been reported in mtGPAT1 knockout mice [20], with decrease in 16:0 (the preferred substrate for mtGPAT1) and increase of 18:0 noted in both liver TAG and phospholipids (PC and PE). To investigate whether acute shRNA-mediated knockdown of mtGPAT1 could result in similar changes in livers of *ob/ob* mice, liver samples from high dose treated mice were evaluated for fatty acid composition. Highly consistent with the findings from knockout mice, reduction of 16:0 and increase of 18:0 were also observed in hepatic neutral lipids and phospholipids of male *ob/ob* mtGPAT1 knockdown mice. Liver TAG of mtGPAT1 knockdown mice contains 27% less 16:0 but 152% more 18:0 compared to control mice treated with GFP-shRNA (Fig. 5A). In liver DAG, the level of 16:0 was significantly reduced by 33% and 18:0 increased by 125% (Fig. 5B), very similar to changes seen for liver TAG. The content of free 16:0 is also decreased (data not shown). In addition, fatty acid composition was comprehensively analyzed in all phospholipid species, including PE, PC, PS, LYPC, SM, and CL. Acute knockdown of mtGPAT1 only reduced the content of 16:0 in PE (Fig. 5C) and CL (Fig. 5D) without affecting other phospholipid species, which is different from the results from mtGPAT1 knockout mice. Our results suggest that mtGPAT1 plays an important role in synthesis of TAG, DAG, PE, and CL in livers of male *ob/ob* mice. Differences seen between hepatic lipid compositions in mtGPAT1 knockout mice and our studies may reflect limited duration of lowered mtGPAT1 activity in our acute knockdown studies, differences between *ob/ob* mice and the strain background of the knockout mice, or differences arising from developmental compensation as a result of complete knockout of mtGPAT1.

Discussion

Mitochondrial GPAT1 has been shown to play an important role in synthesis of glycerolipids, based on a series of elegant gain-of-function studies in hepatocytes and whole animals as well as loss-of function studies in global mtGPAT1 knockout mice [11,14,19–22]. In order to evaluate whether mtGPAT1 could be a therapeutic target for treating obesity and related disorders through pharmacological intervention, we reasoned that alteration of mtGPAT1 activity in developmentally mature obese, diabetic rodents would provide useful information. In this study, adenovirus-mediated RNA interference technology was used to knockdown expression of mtGPAT1 in livers of

Table 2
Gene expression in liver of mtGPAT1 knockdown *ob/ob* mice

Gene	2×10^8 pfu			1×10^9 pfu		
	Vehicle	GFP shRNA	mtGPAT1 shRNA	Vehicle	GFP shRNA	mtGPAT1 shRNA
ACO1	1.05 ± 0.20	1.00 ± 0.17	0.83 ± 0.08	0.94 ± 0.12	1.00 ± 0.36	1.03 ± 0.03
CPT-1a	0.72 ± 0.05	1.00 ± 0.28	0.80 ± 0.10	1.10 ± 0.15	1.00 ± 0.07	1.09 ± 0.07
CPT-II	1.10 ± 0.045	1.00 ± 0.071	0.95 ± 0.039	1.07 ± 0.089	1.00 ± 0.073	1.01 ± 0.088

The expression level of target genes in liver of GFP-shRNA treated mice is arbitrarily set as 1.
Five mice in each group were used for each analysis. Values are presented as means ± standard errors. Expression level of target genes was normalized to 28S rRNA.

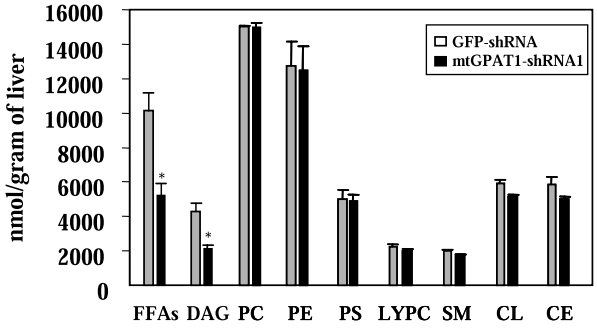

Fig. 4. Lipid analysis in mtGPAT1 knockdown livers. The liver samples of mtGPAT1 knockdown mice and control mice treated with GFP-shRNA virus (high dose 5-day study) were sent to Lipomics Technology Inc. for lipid profiling. The total content of hepatic FFAs, DAG, PC, PE, PS, LYPC, SM, CL, and CE was measured. FFAs, free fatty acids; DAG, diglyceride; PC, phosphatidylcholine; PE, phosphatidylethanolamine; PS, phosphatidylserine; LYPC, lysophosphatidylcholine; SM, sphingomyelin; CL, cardiolipin; CE, cholesterol ester. Student's *t*-test was used to compare statistical differences between liver samples from mice injected with mtGPAT1-shRNA1 and GFP-shRNA, $n = 3$ per group. $^*P < 0.05$.

ob/ob mice, an early on-set obesity/diabetes model with elevated mtGPAT1 expression and activity [11]. This approach allowed a specific assessment of the role for mtGPAT1 in hepatic lipid metabolism of adult obese/diabetic mice and the impact of altered liver metabolism on the systemic lipid profile and other metabolic parameters.

RNA interference is potentially a very powerful means to assess gene function *in vitro* and *in vivo*. Adenoviral delivery of shRNA *in vivo* has been proved to be successful for studying the effects of knocking down genes involved in liver metabolism [23,24]. When adenoviral delivery of shRNA *in vivo* is performed in a disease model in which the target gene expression is increased above normal, knockdown may provide particularly useful information toward understanding the potential of pharmacological intervention. Our results demonstrate that very effective knockdown of mtGPAT1 mRNA was achieved by using adenovirus-mediated RNA interference in liver of *ob/ob* mice, and this was dose dependent. Importantly, it was

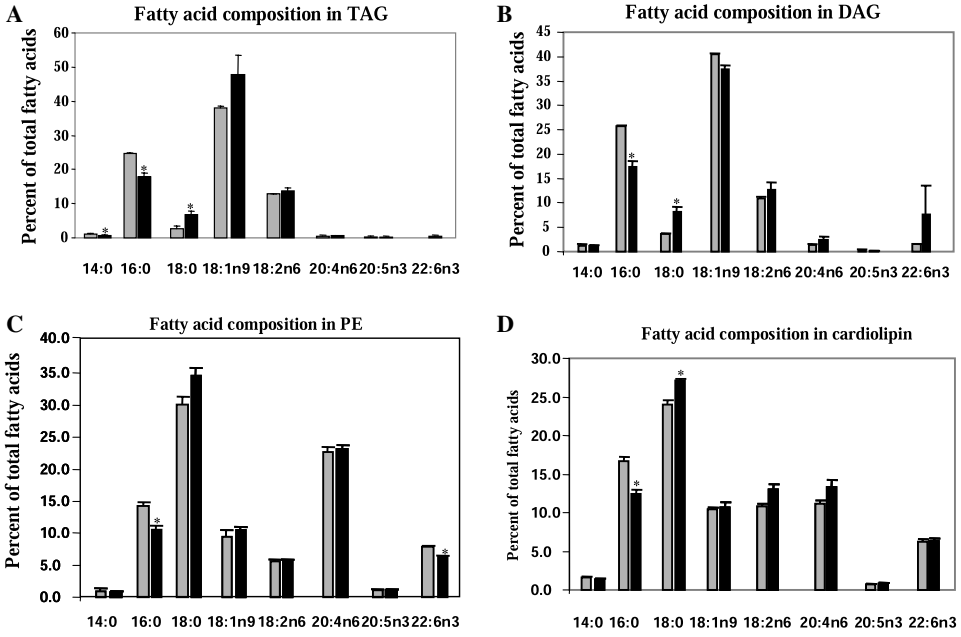

Fig. 5. Fatty acid composition of mtGPAT1 knockdown livers. The liver samples of mtGPAT1 knockdown mice and control mice treated with GFP-shRNA virus (high dose 5-day study) were sent to Lipomics Technology Inc. for fatty acid composition analysis. Data presented in graphs are major fatty acid species. (A) Fatty acid composition in TAG. (B) Fatty acid composition in DAG. (C) Fatty acid composition in PE. (D) Fatty acid composition in cardiolipin. Student's *t*-test was used to compare statistical differences between liver samples from mice injected with mtGPAT1-shRNA1 and GFP-shRNA, $n = 3$ per group. $^*P < 0.05$.

accompanied by robust reductions in mtGPAT1 enzymatic activity.

Knockdown of mtGPAT1 in our studies resulted in robust reduction of hepatic TAG in *ob*/*ob* mice possessing highly steatotic livers. The extent of hepatic lipid reduction was well-correlated with the degree of mtGPAT1 knockdown. This supports the driving role of hepatic mtGPAT1 in the accumulation of liver TAG that subsequently leads to hepatic steatosis. At 5 days after injection of high dose mtGPAT1 shRNA there were also changes in other lipid species. Hepatic DAG and free fatty acid contents were also reduced dramatically. Increased levels of hepatic DAG and FFA are thought to be implicated in development of hepatic insulin resistance and increased hepatic glucose production, through effects on glycogenolysis, gluconeogenesis, glucose release, protein kinase C activation and inflammatory effects [25–29]. The dramatic lowering of hepatic FFA and DAG levels in our mtGPAT1 knockdown *ob*/*ob* mice might thus explain the lowered blood glucose levels seen in the high dose study. This would be a desirable consequence of pharmacological intervention of mtGPAT1 activity. Lowered hepatic DAG content was also reported in mtGPAT1 knockout mice fed a high fat (safflower oil) diet for three weeks, compared with wild-type mice on the same diet [25]. These mice were also protected from development of hepatic insulin resistance, possibly because of lowered DAG-mediated activation of hepatic protein kinase C_ε. We want to point out that our approach only significantly reduced mtGPAT1 activity in liver of *ob*/*ob* mice acutely without affecting mtGPAT1 activity in any other tissue, among which adipose tissue is also an abundant source of this enzyme. This model is very different from mtGPAT1 global knockout mouse model, in which mtGPAT1 is absent in all tissues. Despite this, our observation that plasma TAG levels were not decreased in our male *ob*/*ob* mice is in agreement with observations for male knockout mice [20]; lowered plasma TAG was only observed in female knockout mice, suggesting differences between sexes with respect to storage versus secretion of TAG synthesized via mtGPAT1. Studies using isolated rat hepatocytes that overexpress mtGPAT1 have demonstrated that increased TAG synthesis via mtGPAT1 does not result in increased TAG secretion [14]. It is possible that the lack of effect that we observed on plasma TAG could also imply that TAG synthesis via mtGPAT1 does not significantly impact the pool of TAG directed to secretion rather than storage, at least in male mice. Other explanations, for example compensation through adipose tissue, could also be possible. Our observations of no changes in plasma FFA are also in agreement with observations in mtGPAT1 knockout mice [20].

In contrast to effects on hepatic content of neutral lipids, the total amount of hepatic phospholipids was not affected. Our data indicated that mtGPAT1 preferably directs fatty acids toward synthesis of neutral lipid rather than phospholipid, consistent with existing evidence from mtGPAT1 overexpression in livers of lean mice and with studies on global mtGPAT1 knockout mice [15,19,20]. This is a desirable phenotype since cellular phospholipid levels are important in cell signaling and maintaining the integrity of cell membranes. Plasma cholesterol levels were also lowered with mtGPAT1 knockdown at the higher dose of shRNA for mtGPAT1. This demonstrates that an improved circulating lipid profile results from knockdown of hepatic mtGPAT1 in *ob*/*ob* obese, diabetic mice. The lowered plasma cholesterol is consistent with phenotypes resulting from global mtGPAT1 knockout and liver-directed overexpression of mtGPAT1 [19,20]. It presumably reflects changes in lipoprotein profiles, possibly as a result of decreased triglyceride synthesis in liver. Our studies show that, at least with specific decrease in hepatic mtGPAT1, the effect is specifically on plasma cholesterol esters, while free plasma cholesterol levels are maintained.

It has been hypothesized that mtGPAT1 competes for substrate with CPT1. Therefore, deficiency of mtGPAT1 will direct fatty acids away from lipid synthesis and toward β-oxidation. Despite reported increase of circulating β-hydroxybutyrate levels observed in global mtGPAT1 knockout mice fed on high fat/high sucrose diet or high oil diet [21], no change of plasma β-hydroxybutyrate was observed in our studies. This could be due to the fact that we only knocked down mtGPAT1 in liver for a relatively short duration. Alternatively, high fat content in diet may be necessary to see an increase in plasma β-hydroxybutyrate level associated with mtGPAT1 knockdown, since no difference was reported in chow-fed mtGPAT1 knockout mice compared to control mice [22]. Additionally, our analysis of gene expression for enzymes of mitochondrial and peroxisomal fatty acid oxidation do not provide evidence for increased fatty acid oxidation resulting from mtGPAT1 knockdown in liver.

Palmitoyl-CoA has been reported to be the preferred substrate for mtGPAT1 [30,31], supported by reduction of 16:0 content in liver TAG, PE and PC in female mtGPAT1 knockout mice [20]. Our study provided a comprehensive profiling of hepatic fatty acid composition in neutral lipids and phospholipids with lowered mtGPAT1 expression in obese, diabetic *ob*/*ob* mice, as opposed to in the lean background of the mtGPAT1 knockout mice. We observed reduction of 16:0 and increased 18:0 in liver TAG and PE, and decreased free 16:0, all consistent with changes reported for mtGPAT1 knockout mice. Increased utilization of free 16:0 by other GPATs is ruled out in our study because of unaltered NEM-sensitive GPAT activities in these samples. Additionally, observed reductions of 16:0 content in DAG and cardiolipin shed new light on other lipid pathways that are altered significantly with lowered mtGPAT1 expression in liver. However, unlike mtGPAT1 knockout mice, no change of fatty acid composition was observed in liver PC as a result of hepatic mtGPAT1 knockdown. This may be due to the gender difference of mice used in our study or altered phospholipid metabolism in *ob*/*ob* mice or because total lack of mtGPAT1 activity is required to see this change.

Our results support the interpretation that knockdown of mtGPAT1 in male *ob*/*ob* mice fed a normal chow diet results in a beneficial phenotypic change in glucose metabolism, and is reflected in the reduced hyperglycemia observed with higher extent of mtGPAT1 knockdown. Interestingly, despite the fact that female mtGPAT1 knockout mice have an improved lipid profile and reduced adiposity when fed on normal chow, male mtGPAT1 knockout mice are not resistant to obesity induced by a high fat/high sucrose diet [20,21]. On the contrary, these mice developed glucose intolerance despite increased β-oxidation and decreased liver TAG content. It remains to be been whether female mice would have a similar response when placed on a high fat/high sucrose diet. An explanation for the development of glucose intolerance in male mtGPAT1 knockout mice is that it is due to the high load of sucrose rather than the high fat content in the diet. Increased fatty acid oxidation in the absence of mtGPAT1 may shift the balance of energy metabolism towards lipid utilization, therefore making carbohydrate utilization vulnerable to an extra load. Indeed, mtGPAT1 knockout mice fed on a diet comprising high fat only demonstrated improved hepatic insulin sensitivity and whole body glucose tolerance [22].

In summary, our studies demonstrate that knockdown of mtGPAT1 in livers of *ob*/*ob* mice via adenovirus-mediated RNA interference was effective and resulted in significantly reduced liver TAG, DAG and FFA content, decreased plasma cholesterol ester levels, and reduced hyperglycemia. Since the RNAi approach is similar to pharmacological intervention, our data suggest that small molecule inhibitors of mtGPAT1 may be beneficial for correcting obesity related disorders.

References

[1] P. Zimmet, K.G. Alberti, J. Shaw, Global and societal implications of the diabetes epidemic, Nature 414 (2001) 782–787.

[2] P.G. Kopelman, Obesity as a medical problem, Nature 404 (2000) 635–643.

[3] H.S. Sul, D. Wang, Nutritional and hormonal regulation of enzymes in fat synthesis: studies of fatty acid synthase and mitochondrial glycerol-3-phosphate acyltransferase gene transcription, Annu. Rev. Nutr. 18 (1998) 331–351.

[4] Y. Shi, P. Burn, Lipid metabolic enzymes: emerging drug targets for the treatment of obesity, Nat. Rev. Drug Discov. 3 (2004) 695–710.

[5] L.N. Daae, J. Bremer, The acylation of glycerophosphate in rat liver. A new assay procedure for glycerophosphate acylation, studies on its subcellular and submitochondrial localization and determination of the reaction products, Biochim. Biophys. Acta 210 (1970) 92–104.

[6] T.M. Lewin, N.M. Schwerbrock, D.P. Lee, R.A. Coleman, Identification of a new glycerol-3-phosphate acyltransferase isoenzyme, mtGPAT2, in mitochondria, J. Biol. Chem. 279 (2004) 13488–13495.

[7] D.H. Shin, J.D. Paulauskis, N. Moustaid, H.S. Sul, Transcriptional regulation of p90 with sequence homology to *Escherichia coli* glycerol-3-phosphate acyltransferase, J. Biol. Chem. 266 (1991) 23834–23839.

[8] T.M. Lewin, D.A. Granger, J.H. Kim, R.A. Coleman, Regulation of mitochondrial sn-glycerol-3-phosphate acyltransferase activity: response to feeding status is unique in various rat tissues and is discordant with protein expression, Arch. Biochem. Biophys. 396 (2001) 119–127.

[9] L.K. Dircks, H.S. Sul, Mammalian mitochondrial glycerol-3-phosphate acyltransferase, Biochim. Biophys. Acta 1348 (1997) 17–26.

[10] R.A. Coleman, D.P. Lee, Enzymes of triacylglycerol synthesis and their regulation, Prog. Lipid Res. 43 (2004) 134–176.

[11] D. Linden, L. William-Olsson, M. Rhedin, A.K. Asztely, J.C. Clapham, S. Schreyer, Overexpression of mitochondrial GPAT in rat hepatocytes leads to decreased fatty acid oxidation and increased glycerolipid biosynthesis, J. Lipid Res. 45 (2004) 1279–1288.

[12] S.C. Jamdar, W.F. Cao, Triacylglycerol biosynthetic enzymes in lean and obese Zucker rats, Biochim. Biophys. Acta 1255 (1995) 237–243.

[13] Y. Lee, H. Hirose, Y.T. Zhou, V. Esser, J.D. McGarry, R.H. Unger, Increased lipogenic capacity of the islets of obese rats: a role in the pathogenesis of NIDDM, Diabetes 46 (1997) 408–413.

[14] T.M. Lewin, S. Wang, C.A. Nagle, C.G. Van Horn, R.A. Coleman, Mitochondrial glycerol-3-phosphate acyltransferase-1 directs the metabolic fate of exogenous fatty acids in hepatocytes, Am. J. Physiol. Endocrinol. Metab. 288 (2005) E835–E844.

[15] R.A. Igal, S. Wang, M. Gonzalez-Baro, R.A. Coleman, Mitochondrial glycerol phosphate acyltransferase directs the incorporation of exogenous fatty acids into triacylglycerol, J. Biol. Chem. 276 (2001) 42205–42212.

[16] M.R. Gonzalez-Baro, D.A. Granger, R.A. Coleman, Mitochondrial glycerol phosphate acyltransferase contains two transmembrane domains with the active site in the N-terminal domain facing the cytosol, J. Biol. Chem. 276 (2001) 43182–43188.

[17] H. Park, V.K. Kaushik, S. Constant, M. Prentki, E. Przybytkowski, N.B. Ruderman, A.K. Saha, Coordinate regulation of malonyl-CoA decarboxylase, sn-glycerol-3-phosphate acyltransferase, and acetyl-CoA carboxylase by AMP-activated protein kinase in rat tissues in response to exercise, J. Biol. Chem. 277 (2002) 32571–32577.

[18] D.M. Muoio, K. Seefeld, L.A. Witters, R.A. Coleman, AMP-activated kinase reciprocally regulates triacylglycerol synthesis and fatty acid oxidation in liver and muscle: evidence that sn-glycerol-3-phosphate acyltransferase is a novel target, Biochem. J. 338 (Pt. 3) (1999) 783–791.

[19] D. Linden, L. William-Olsson, A. Ahnmark, K. Ekroos, C. Hallberg, P. Sjogren, B. Becker, L. Svensson, J.C. Clapham, J. Oscarsson, S. Schreyer, Liver-directed overexpression of mitochondrial glycerol-3-phosphate acyltransferase results in hepatic steatosis, increased triacylglycerol secretion and reduced fatty acid oxidation, FASEB J. 20 (2006) 434–443.

[20] L.E. Hammond, P.A. Gallagher, S. Wang, S. Hiller, K.D. Kluckman, E.L. Posey-Marcos, N. Maeda, R.A. Coleman, Mitochondrial glycerol-3-phosphate acyltransferase-deficient mice have reduced weight and liver triacylglycerol content and altered glycerolipid fatty acid composition, Mol. Cell Biol. 22 (2002) 8204–8214.

[21] L.E. Hammond, S. Neschen, A.J. Romanelli, G.W. Cline, O.R. Ilkayeva, G.I. Shulman, D.M. Muoio, R.A. Coleman, Mitochondrial glycerol-3-phosphate acyltransferase-1 is essential in liver for the metabolism of excess acyl-CoAs, J. Biol. Chem. 280 (2005) 25629–25636.

[22] S. Neschen, K. Morino, L.E. Hammond, D. Zhang, Z.X. Liu, A.J. Romanelli, G.W. Cline, R.L. Pongratz, X.M. Zhang, C.S. Choi, R.A. Coleman, G.I. Shulman, Prevention of hepatic steatosis and hepatic insulin resistance in mitochondrial acyl-CoA:glycerol-sn-3-phosphate acyltransferase 1 knockout mice, Cell Metab. 2 (2005) 55–65.

[23] S.H. Koo, L. Flechner, L. Qi, X. Zhang, R.A. Screaton, S. Jeffries, S. Hedrick, W. Xu, F. Boussouar, P. Brindle, H. Takemori, M. Montminy, The CREB coactivator TORC2 is a key regulator of fasting glucose metabolism, Nature 437 (2005) 1109–1111.

[24] C.M. Taniguchi, K. Ueki, R. Kahn, Complementary roles of IRS-1 and IRS-2 in the hepatic regulation of metabolism, J. Clin. Invest. 115 (2005) 718–727.

[25] J.J. Bahl, M. Matsuda, R.A. DeFronzo, R. Bressler, In vitro and in vivo suppression of gluconeogenesis by inhibition of pyruvate carboxylase, Biochem. Pharmacol. 53 (1997) 67–74.

[26] J.R. Williamson, R.A. Kreisberg, P.W. Felts, Mechanism for the stimulation of gluconeogenesis by fatty acids in perfused rat liver, Proc. Natl. Acad. Sci. USA 56 (1966) 247–254.
[27] D. Massillon, N. Barzilai, M. Hawkins, D. Prus-Wertheimer, L. Rossetti, Induction of hepatic glucose-6-phosphatase gene expression by lipid infusion, Diabetes 46 (1997) 153–157.
[28] G. Boden, P. She, M. Mozzoli, P. Cheung, K. Gumireddy, P. Reddy, X. Xiang, Z. Luo, N. Ruderman, Free fatty acids produce insulin resistance and activate the proinflammatory nuclear factor-kappaB pathway in rat liver, Diabetes 54 (2005) 3458–3465.
[29] G. Boden, L.H. Carnell, Nutritional effects of fat on carbohydrate metabolism, Best Pract. Res. Clin. Endocrinol. Metab. 17 (2003) 399–410.
[30] A. Vancura, D. Haldar, Purification and characterization of glycerophosphate acyltransferase from rat liver mitochondria, J. Biol. Chem. 269 (1994) 27209–27215.
[31] S.F. Yet, Y.K. Moon, H.S. Sul, Purification and reconstitution of murine mitochondrial glycerol-3-phosphate acyltransferase. Functional expression in baculovirus-infected insect cells, Biochemistry 34 (1995) 7303–7310.